Probing Pore Wetting in Membrane Distillation Using Impedance: Early Detection and Mechanism of Surfactant-Induced Wetting

Yuanmiaoliang Chen,[†] Zhangxin Wang,[†] G. Kane Jennings,[‡] and Shihong Lin*,[†,‡]

[†]Department of Civil and Environmental Engineering, Vanderbilt University, Nashville, Tennessee 37235-1831, United States
[‡]Department of Chemical and Biomolecular Engineering, Vanderbilt University, Nashville, Tennessee 37235-1604, United States

S *Supporting Information*

ABSTRACT: Pore wetting is an important failure mechanism unique to membrane distillation (MD). The existing approach of wetting detection based on distillate conductivity works only when a membrane has failed in the presence of fully wicked-through pores. In this study, we develop a novel and simple method, based on measurement of cross-membrane impedance, for monitoring the dynamics of membrane pore wetting and enabling early detection of imminent wetting-based membrane failure. Using Triton X-100 to induce pore wetting in direct contact MD experiments, we demonstrated the rapid response of single-frequency impedance to partial pore wetting long before any change in distillate conductivity was observed. We also conducted an MD experiment using alternating feed solutions with and without surfactants to elucidate the mechanism of surfactant-induced pore wetting. Our experimental observations suggest that surfactant-induced pore wetting occurred via progressive movement of the water–air interface and that adsorption of surfactants to the membrane pore surface plays an important role in controlling the kinetics of progressive wetting.
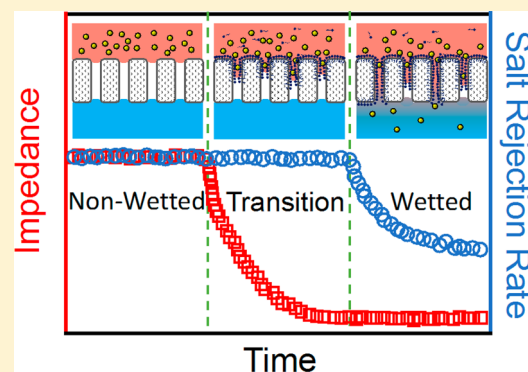
INTRODUCTION

Membrane distillation (MD) is a membrane-based thermal desalination process.[1−4] In a typical MD system, a microporous hydrophobic membrane is employed to separate a hot salty stream (feed solution) and a cold distillate stream. The temperature difference between the feed and distillate streams creates a partial vapor-pressure difference that drives the water vapor from the feed solution to the distillate. The hydrophobicity of the membrane prevents direct liquid permeation of the feed solution, which is essential for solute rejection. Compared to pressure-driven membrane processes, such as reverse osmosis (RO), MD has several major technological advantages.[5−10] First, MD can desalinate highly saline brine, the osmotic pressure of which far exceeds the operating pressure of RO, the state-of-the-art desalination process. Second, MD is capable of utilizing low-grade thermal energy such as solar thermal energy, geothermal energy, and industrial waste heat. Last but not least, the capital cost of MD is low because of the absence of any high-pressure and high-temperature components. Because of these advantages, MD has recently been proposed as a promising candidate for on-site desalination of highly challenging wastewater, such as shale gas/oil-produced water.[9,11−14]

Despite these promising aspects of MD, its large-scale practical application is still limited because of certain technical challenges. One prominent challenge unique to MD is membrane wetting.[15−17] Membrane wetting refers to the direct liquid permeation of a salty feed solution through membrane pores, which results in compromised salt rejection and thus process

failure. Certain substances have been shown to be very effective in inducing MD membrane wetting, such as amphiphilic molecules (e.g., surfactants and proteins) and low-surface tension liquids (e.g., alcohols).[11,18−20] In addition, mineral crystallization in membrane pores,[21−23] chemical degradation of membrane materials,[24] and the usage of anti-scalants have also been found to promote wetting.[25] The prevention of membrane pore wetting is of critical importance in MD, especially when applied for the treatment of feedwater with complex compositions.

The conventional approach of wetting detection is by monitoring the electrical conductivity of the distillate.[26,27] Despite its simplicity and prevalent use, this conductivity-based approach can detect wetting only when certain pores have been penetrated and the MD membrane has already failed. Recently, an alternative wetting detection technique based on measuring the direct current across a conductive MD membrane was proposed.[28] While this approach appears to be more sensitive than measuring distillate conductivity for monitoring the onset of membrane wetting, it still cannot detect imminent wetting of membrane pores that have not yet been wicked through. A novel monitoring approach that can provide effective early detection of imminent membrane wetting is highly desirable, as it may
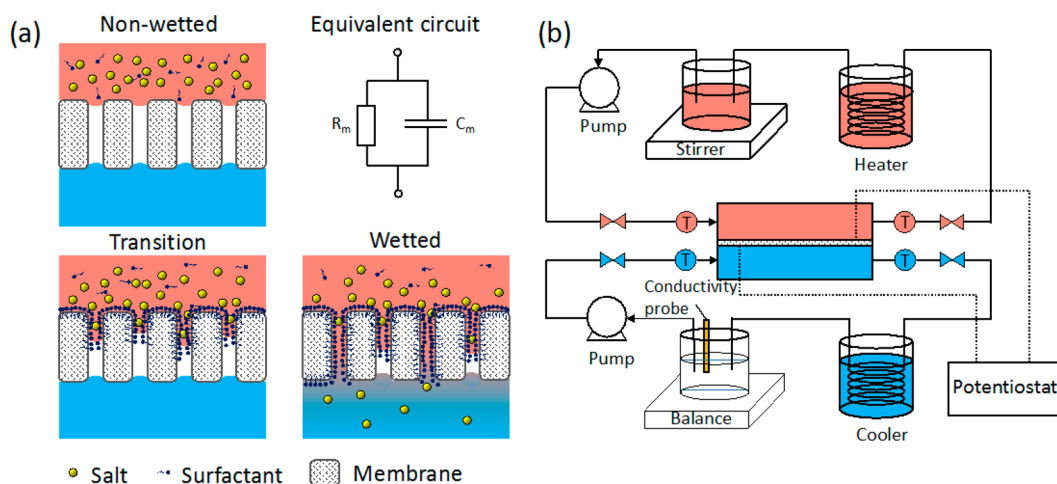
Figure 1. (a) Illustration of the possible membrane pore wetting states and corresponding equivalent circuit for impedance-based monitoring. The equivalent circuit captures only the region of the MD membrane with air pockets and does not consider contributions to impedance at and outside the membrane−solution interfaces. (b) Schematic of a DCMD system equipped with in situ impedance measurement capability.

potentially enable the implementation of timely measures to prevent process failure due to wetting.

Electrochemical impedance spectroscopy (EIS) is a versatile characterization technique that probes the magnitude and phase of the electrochemical impedance of a system. It works by measuring the electrical response of a system upon application of alternating potentials with a wide spectrum of frequencies.[29,30] Recently, EIS has been utilized to determine the wetting state of textured surfaces, taking advantage of the fact that the impedance varies depending on whether the grooves (or pores) of a rough (or porous) surface are filled with an electrolyte solution or air.[31−33] Similarly, EIS has also recently been utilized to construct a novel porometry for characterizing pore size distribution of microporous membranes.[34] In addition, several studies about the successful implementation of EIS to monitor fouling in membrane systems such as RO, microfiltration, and forward osmosis (FO) have been reported.[29,35−41] Through the use of EIS, early detection of RO membrane fouling has been achieved.[29,42] The mechanisms of various types of membrane fouling have also been investigated using EIS.[29,36,37,43,44] MD differs from all these membrane processes in that pores in a functional MD membrane should always be filled with air. These air-filled pores, sandwiched by the feed solution and distillate, comprise an equivalent capacitor for which impedance-based characterization is strongly relevant. Surprisingly, however, no impedance-based study of MD pore wetting has been reported.

This study explores the use of an impedance-based technique to monitor pore wetting in MD. Here, we construct a direct contact MD (DCMD) system with the capability of in situ impedance measurement and use such a system to investigate the dynamics of surfactant-induced pore wetting. Specifically, we perform DCMD experiments with a commercial hydrophobic polyvinylidene fluoride (PVDF) membrane and induce pore wetting by adding surfactants to the feed solution. Two real-time monitoring techniques, one based on single-frequency, cross-membrane impedance and the other based on distillate conductivity, are employed and compared in probing membrane pore wetting. Finally, we also employ these two techniques coupled with a carefully designed experimental scheme using alternating feed solutions to investigate the possible mechanism of dynamic pore wetting.

MATERIALS AND METHODS

Principle and Experimental Setup of Impedance-Based Wetting Monitoring. In an MD process, the pores in the microporous membrane have three possible wetting states: the nonwetted state, the transition state, and the wetted state (Figure 1a). In the nonwetted state, the membrane pores are fully filled with air.[45] According to the literature,[31,32] the air-filled microporous membrane can be modeled as a parallel circuit of a resistor and a capacitor when considering its impedance. Specifically, the polymeric membrane material and the air-filled pores between the two liquid−air interfaces constitute the resistor and the capacitor, respectively.

In the presence of surfactant molecules in the feed solution, the feed solution can partially penetrate the air-filled pores (i.e., the transition state). This partial penetration of the feed solution decreases the average distance between the two liquid−air interfaces, or the thickness of the air gap within the pores, which consequently increases the capacitance of the air pocket and reduces the resistance of the polymeric membrane, both leading to a reduction of the overall system impedance (at a given frequency). If such a picture of partial wetting without pore breakthrough is true, one should expect the observation of reduced impedance but no change in distillate salinity, as the pores have not yet been penetrated to become available channels for direct permeation of the feed solution.

As surfactant-induced wetting proceeds further, some membrane pores are eventually fully penetrated (i.e., the wetted state),[45] in which case the salt in the feed solution can freely move through the wetted pores and thereby significantly undermine the salt rejection of the MD process. In this wetted state, the equivalent capacitor is short-circuited by the wicked-through pores, leading to a drastic decrease in the overall impedance. The final system impedance in the wetted state is expected to be negligible compared to the initial impedance as the resistance due to the wetted pores is negligible compared to the capacitive contribution to the overall impedance.

Following this principle, a DCMD system with the capability of measuring impedance in the wetting experiments is shown in Figure 1b. A commercial hydrophobic PVDF membrane coupon of 8 cm × 2.5 cm (GE Health Life Sciences, Pittsburgh, PA) was used in this study. The nominal pore size and average thickness of the membrane are 0.45 and 170 μm, respectively. In all DCMD

experiments, a 0.6 M NaCl solution was used as the feed solution and deionized water was used as the distillate. The influent temperatures of feed and distillate streams were maintained at 60 and 20 °C, respectively. The hydraulic pressure of the feed stream was kept higher than that of the distillate stream to facilitate unequivocal detection of membrane pore wetting that will be reflected by the increased salinity of the distillate.[5,11,46,47]

A potentiostat (SP-150, BioLogic Science) was coupled with the DCMD system to conduct in situ measurement of the impedance across the membrane during MD. Two titanium electrodes (1 cm × 0.5 cm) were placed in direct contact with the two sides of the MD membrane. To identify a suitable operational frequency for time-resolved impedance measurement, a frequency scan was first conducted in an operating DCMD system. On the basis of the results of the frequency scan, we chose 100 kHz as the operational frequency for measuring time-resolved impedance (justifications given in the Supporting Information).

Surfactant-Induced Membrane Wetting Experiments. For each membrane wetting experiment, the time-resolved impedance and the salt rejection rate of the membrane were both monitored. Cross-membrane impedance at a single frequency of 100 kHz was measured over time to probe the dynamics of membrane wetting. Real-time salt rejection of the membrane was obtained from real-time water flux and distillate conductivity. In each wetting experiment, the system was first operated with a feed solution free of surfactants to establish a stable baseline for flux. After ~30 min, a different amount of Triton X-100 was added to adjust the surfactant concentration of the feed solution to 10 and 25 ppm in two separate experiments conducted to investigate the impact of surfactant concentration on wetting kinetics. We also measured the surface tension of these feed solutions with 10 and 25 ppm Triton X-100, in the presence of 0.6 M NaCl and at 60 °C, using the drop shape analysis method.

To further understand the mechanism of membrane wetting caused by surfactants, we conducted another membrane wetting experiment with alternating feed solutions with and without Triton X-100. The concentration of Triton X-100 after addition was maintained at 10 ppm. Once a 15% decline in membrane impedance was detected with a surfactant-dosed feed solution, we rinsed the PVDF membrane with deionized (DI) water and replaced the surfactant-dosed feed solution with a surfactant-free feed solution. This process was repeated for three cycles.

■ RESULTS AND DISCUSSION

Impedance Enables Early Detection of Wetting. With a surfactant-free feed solution, both constant impedance and perfect salt rejection were observed (Figure 2a,b), indicating that the PVDF membrane was in a nonwetted state (Figure 1a). Soon after the addition of surfactants, the impedance began to decrease, whereas the salt rejection remained almost perfect until the impedance became negligibly small. This stage marked by decreasing impedance suggests the system to be in a transition state of membrane wetting (Figure 1a). In this state, the impedance was constantly reduced as the feed solution−air interface gradually propagated toward the distillate. However, because the membrane pores were not yet wicked through by the feed solution in this transition state, the partially air-filled membrane pores still served as a barrier for direct liquid permeation and maintained a near-perfect salt rejection. In addition, the normalized water flux remained at unity during this transition stage (Figure S2), again supporting the argument that none of the pores were fully penetrated.
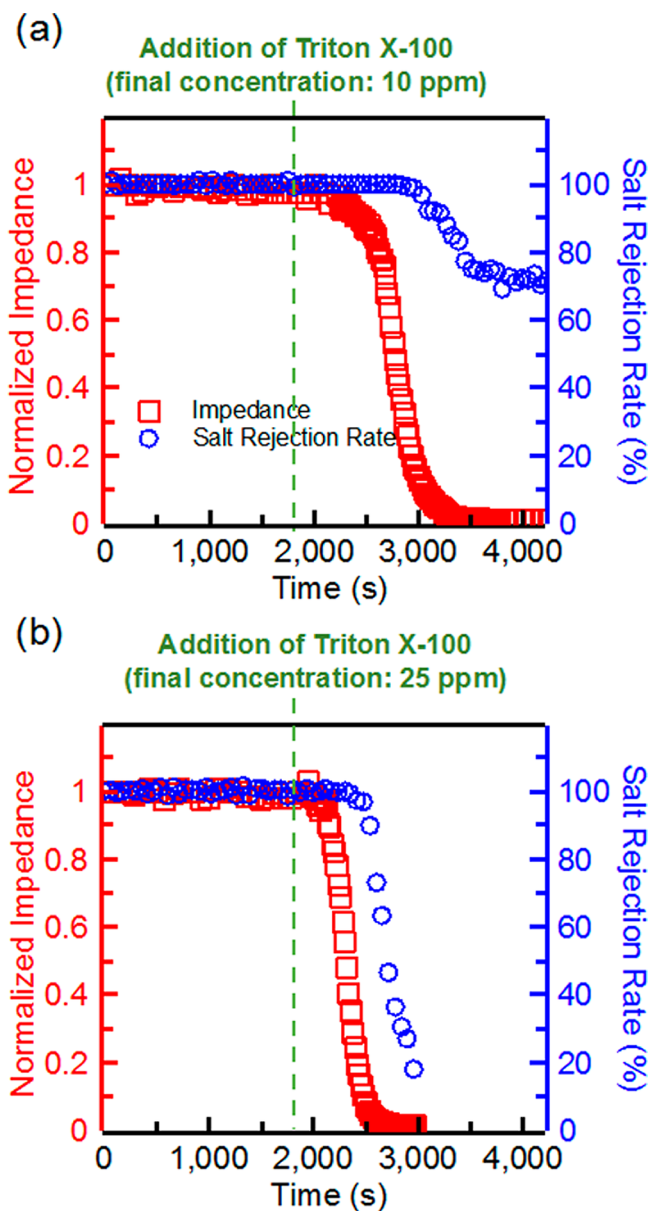

Figure 2. Impedance (red squares, left Y-axis) across the PVDF membrane and salt rejection rate (blue circles, right Y-axis) in DCMD experiments in the presence of (a) 10 ppm Triton X-100 and (b) 25 ppm Triton X-100. The impedances are normalized by the initial impedances of the respective measurements (4740 and 4800 Ω for panels a and b, respectively). We note that detection of the change in conductivity in the distillate reservoir was delayed for the time required for the distillate stream to exit the DCMD system. However, such a delay is calculated to be <26 s and negligible compared to the delay between the onsets of decreases in impedance and conductivity shown in these figures. The real-time water fluxes in these two experiments are shown in Figure S2.

Eventually, the feed solution penetrated through some membrane pores, resulting in a noticeable drop in the salt rejection rate. Such a drop in the salt rejection rate, however, was not observed until the impedance became negligibly small. The time difference between the onsets of impedance reduction and salt rejection rate reduction represents the duration of the transition state in a membrane pore wetting process. Even with these surfactant-containing feed solutions of a relatively strong wetting propensity, such a delay was still quite significant (Figure 2). Therefore, this impedance-based technique, capable of
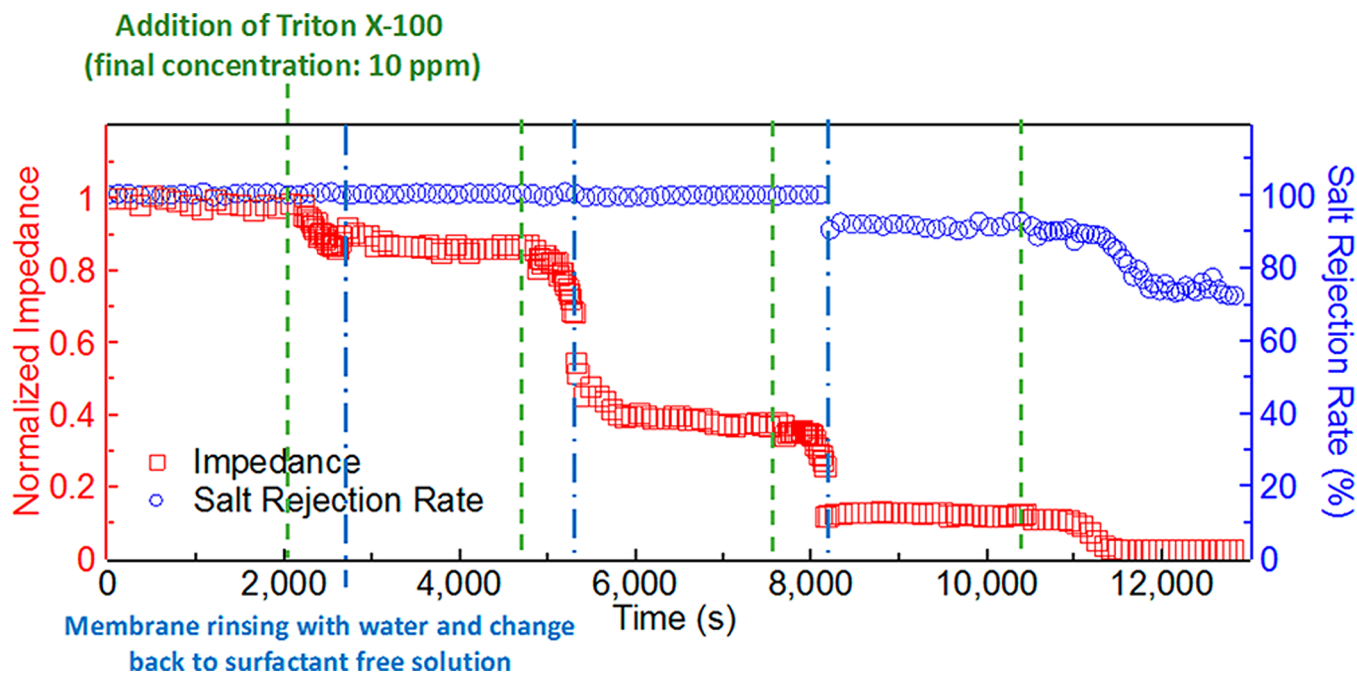
Figure 3. Impedance (red squares, left *Y*-axis) across the PVDF membrane and salt rejection rate (blue circles, right *Y*-axis) in DCMD experiments with alternating feed solutions. The green dashed lines indicate the addition of Triton X-100, which resulted in a feed solution with 10 ppm Triton X-100. The blue dashed−dotted lines indicate the points at which the membrane surface was rinsed with DI water, followed by replacement of the surfactant-containing feed solution with a surfactant-free feed solution of the same salinity. Such a cycle comprising surfactant dosing, membrane rinsing, and feed solution replacement was repeated for multiple cycles. The water flux in this experiment is shown in Figure S3 in the Supporting Information.

capturing the transition state, can be utilized for early detection of membrane wetting before any pore is completely wicked through.

The duration of the transition state strongly depends on the surfactant concentration. In the experiments with feed solutions containing 10 and 25 ppm Triton X-100, the delays of complete pore wetting were observed to be ~1000 and ~500 s, respectively. In addition, the surfactant concentration also had a significant impact on the final salt rejection rate in the wetted state. While the salt rejection dropped to <20% with 25 ppm Triton X-100, it was only reduced to ~75% with 10 ppm Triton X-100.

Mechanism of Dynamic Wetting by a Surfactant-Dosed Feed Solution. The criterion for maintaining a nonwetted state is that the hydraulic pressure is lower than the liquid entry pressure (LEP) as given by eq 1:

$$\text{LEP} = -2\frac{B\gamma_{L}\cos\theta_{0}}{r} \tag{1}$$

where γ_{L} is the liquid surface tension, θ_{0} is the intrinsic liquid contact angle (CA) with the membrane materials (not the apparent CA), r is the pore radius, and B is a geometric factor accounting for noncylindrical pores. The presence of surfactants reduces both γ_{L} and θ_{0}, thereby lowering the LEP and causing intrusion of the feed solution into the pores.[2,19,46,48,49] On the other hand, surfactants also adsorb to the pore surface via the attractive interaction between the hydrophobic tails of the surfactants and the hydrophobic pore surface. While adsorption of surfactants can reduce the surface tension of membrane pores, it does not occur until the pore surface is wetted by the surfactant-containing solution; i.e., surfactants cannot attach to the dry region of a pore to make it hydrophilic and thereby facilitate further pore wetting. Consequently, a decrease in membrane surface tension by surfactant adsorption cannot

explain the progressive, instead of instant, propagation of the liquid−air interface.

Previous studies of capillary imbibition with surfactant solutions suggest that the adsorption of the surfactant to the capillary surface reduces the kinetic rate of pore wicking.[50−52] In the case of MD wetting, the rapid adsorption of surfactants to the wetted pore region depletes the surfactant at the liquid−air interface and thus significantly mitigates the effect of surfactants on reducing γ_{L}. In other words, the γ_{L} at the liquid−air interface is higher than the γ_{L} of the bulk solution because of the reduced surfactant concentration at the liquid−air interface. After initial pore intrusion, the characteristic length for diffusion of the surfactant to the pore surface (i.e., surfactant depletion) is significantly smaller than that for diffusion of the surfactant from the bulk solution to the liquid−air interface (i.e., surfactant replenishment). Therefore, the gradual propagation of liquid air is kinetically limited by the bulk-to-interface diffusion of surfactants. In other words, surfactant adsorption does not promote progressive wetting by rendering the pores hydrophilic but rather deters instant wetting by maintaining a moderate surface tension near the liquid−air interface, which in turn results in progressive wetting.

This theory of a higher γ_{L} near the liquid−air interface (than that in the bulk), widely accepted for capillary imbibition, is also supported by our observation that the feed solution with 25 ppm Triton X-100 wetted the membrane much faster than that with 10 ppm Triton X-100 (Figure 2). We note that the surface tensions of the feed solutions with 10 and 25 ppm Triton X-100 were measured to be 26.85 ± 0.19 and 27.10 ± 0.29 mN/m, respectively, as high salinity and temperature both reduced the critical micelle concentration and the surface tension of the surfactant solution.[53,54] The feed solution with a higher concentration of Triton X-100 was kinetically favored in wetting the hydrophobic membrane, not because it imparted a lower

surface tension to the feed solution but because it sustained a larger concentration gradient for diffusion of surfactants from the bulk to the liquid−air interface.

Because surfactants were continuously removed from the feed solution in the pore, if the source for surfactant replenishment was removed, progressive wetting would stop. To support this argument, MD experiments with alternating feed solutions with and without surfactants were conducted, and the results are presented in Figure 3. The addition of 10 ppm Triton X-100 reduced the impedance, similar to what is presented in Figure 2a. Rinsing the membrane with DI water and replacing the feed solution with a surfactant-free saline feed solution stopped the decline of impedance, because the source for replenishing the surfactant at the liquid−air interface was no longer available.

After three cycles of operations with a feed solution containing Triton X-100, certain membrane pores were eventually wicked through and salt rejection was finally compromised. Upon the fourth operation with a surfactant-containing feed solution, the impedance became negligibly small, and the salt rejection rate further dropped to 70% (unacceptably low for MD applications). In this wetted state, a fraction of the pores was fully wicked through whereas the rest of the pores remained partially wetted but not wicked through.

Implications. The impedance-based technique for probing pore wetting in DCMD can be a powerful tool for in situ monitoring of the wetting state of operating DCMD systems. The ability to identify the transition state, in which none of the pores is fully wicked through, makes possible the early detection of imminent membrane failure. Such early detection may potentially lead to the development of effective measures that can prevent the operational failure of a DCMD system in a timely manner. For instance, results from Figure 3 suggest that if one removes surface active agents soon after a decline in impedance is observed, membrane wetting in MD can be effectively prevented.

In addition to the potential practical benefit of wetting management, this novel impedance-based technique also provides tremendous insight in unveiling the dynamics and mechanism of pore wetting in DCMD processes. The existing method of monitoring distillate salinity for wetting detection is straightforward but sheds limited light on the dynamic process of wetting. Here, for example, the impedance technique reveals that pore wetting induced by Triton X-100 is a progressive process with gradual movement of the liquid−air interface, instead of one in which parts of the pores are instantly wicked through. Our results also suggest that, similar to capillary imbibition, adsorption of surfactants to the pore surface plays a critical role in deterring wetting. We expect this impedance technique, when coupled with well-designed experimental schemes, can lead to new opportunities to understand the impacts of chemical composition, concentration, and other operating conditions on the dynamics of pore wetting in MD.

■ ASSOCIATED CONTENT

Ⓢ Supporting Information

The Supporting Information is available free of charge on the ACS Publications website at DOI: 10.1021/acs.estlett.7b00372.

Details about EIS frequency scan and water fluxes in MD experiments (PDF)

■ AUTHOR INFORMATION

Corresponding Author

*E-mail: shihong.lin@vanderbilt.edu. Telephone: +1 (615) 322-7226.

ORCID Ⓘ

G. Kane Jennings: 0000-0002-3531-7388

Shihong Lin: 0000-0001-9832-9127

Author Contributions

Y.C. and Z.W. contributed equally to this work.

Notes

The authors declare no competing financial interest.

■ REFERENCES

(1) Lawson, K. W.; Lloyd, D. R. Membrane Distillation. *J. Membr. Sci.* **1997**, *124*, 1−25.

(2) Alkhudhiri, A.; Darwish, N.; Hilal, N. Membrane Distillation: A Comprehensive Review. *Desalination* **2012**, *287*, 2−18.

(3) Drioli, E.; Ali, A.; Macedonio, F. Membrane Distillation: Recent Developments and Perspectives. *Desalination* **2015**, *356*, 56−84.

(4) Khayet, M.; Matsuura, T.; Mengual, J. I.; Qtaishat, M. Design of Novel Direct Contact Membrane Distillation Membranes. *Desalination* **2006**, *192*, 105−111.

(5) Wang, Z.; Lin, S. Membrane Fouling and Wetting in Membrane Distillation and Their Mitigation by Novel Membranes with Special Wettability. *Water Res.* **2017**, *112*, 38−47.

(6) Banat, F.; Jwaied, N. Economic Evaluation of Desalination by Small-Scale Autonomous Solar-Powered Membrane Distillation Units. *Desalination* **2008**, *220*, 566−573.

(7) Bundschuh, J.; Ghaffour, N.; Mahmoudi, H.; Goosen, M.; Mushtaq, S.; Hoinkis, J. Low-Cost Low-Enthalpy Geothermal Heat for Freshwater Production: Innovative Applications Using Thermal Desalination Processes. *Renewable Sustainable Energy Rev.* **2015**, *43*, 196−206.

(8) Kim, Y. D.; Thu, K.; Ghaffour, N.; Choon Ng, K. Performance Investigation of a Solar-Assisted Direct Contact Membrane Distillation System. *J. Membr. Sci.* **2013**, *427*, 345−364.

(9) Shaffer, D. L.; Arias Chavez, L. H.; Ben-Sasson, M.; Romero-Vargas Castrillón, S.; Yip, N. Y.; Elimelech, M. Desalination and Reuse of High-Salinity Shale Gas Produced Water: Drivers, Technologies, and Future Directions. *Environ. Sci. Technol.* **2013**, *47*, 9569−9583.

(10) Martinetti, C. R.; Childress, A. E.; Cath, T. Y. High Recovery of Concentrated RO Brines Using Forward Osmosis and Membrane Distillation. *J. Membr. Sci.* **2009**, *331*, 31−39.

(11) Lin, S.; Nejati, S.; Boo, C.; Hu, Y.; Osuji, C. O.; Elimelech, M. Omniphobic Membrane for Robust Membrane Distillation. *Environ. Sci. Technol. Lett.* **2014**, *1*, 443−447.

(12) Camacho, L. M.; Dumée, L.; Zhang, J.; Li, J. De.; Duke, M.; Gomez, J.; Gray, S. Advances in Membrane Distillation for Water Desalination and Purification Applications. *Water (Basel, Switz.)* **2013**, *5*, 94−196.

(13) Gregory, K. B.; Vidic, R. D.; Dzombak, D. a. Water Management Challenges Associated with the Production of Shale Gas by Hydraulic Fracturing. *Elements* **2011**, *7*, 181−186.

(14) Warner, N. R.; Christie, C. a.; Jackson, R. B.; Vengosh, A. Impacts of Shale Gas Wastewater Disposal on Water Quality in Western Pennsylvania. *Environ. Sci. Technol.* **2013**, *47*, 11849−11857.

(15) Qtaishat, M. R.; Matsuura, T. Modelling of Pore Wetting in Membrane Distillation Compared with Pervaporation. In *Pervaportion, Vapour Permeation and Membrane Distillation: Principles and Applications*; Basile, A., Figoli, A., Khayet, M., Eds.; Elsevier, Woodhead: Waltham, MA, 2015; pp 385−413.

(16) Guillen-Burrieza, E.; Mavukkandy, M. O.; Bilad, M. R.; Arafat, H. A. Understanding Wetting Phenomena in Membrane Distillation and How Operational Parameters Can Affect It. *J. Membr. Sci.* **2016**, *515*, 163–174.

(17) Liao, Y.; Wang, R.; Fane, A. G. Engineering Superhydrophobic Surface on Poly(vinylidene Fluoride) Nanofiber Membranes for Direct Contact Membrane Distillation. *J. Membr. Sci.* **2013**, *440*, 77–87.

(18) Kargbo, D. M.; Wilhelm, R. G.; Campbell, D. J. Natural Gas Plays in the Marcellus Shale: Challenges and Potential Opportunities. *Environ. Sci. Technol.* **2010**, *44*, 5679–5684.

(19) Franken, A. C. M.; Nolten, J. A. M.; Mulder, M. H. V.; Bargeman, D.; Smolders, C. A. Wetting Criteria for the Applicability of Membrane Distillation. *J. Membr. Sci.* **1987**, *33*, 315–328.

(20) Rezaei, M.; Warsinger, D. M.; Lienhard V, J. H.; Samhaber, W. M. Wetting Prevention in Membrane Distillation through Superhydrophobicity and Recharging an Air Layer on the Membrane Surface. *J. Membr. Sci.* **2017**, *530*, 42–52.

(21) Nghiem, L. D.; Cath, T. A Scaling Mitigation Approach during Direct Contact Membrane Distillation. *Sep. Purif. Technol.* **2011**, *80*, 315–322.

(22) Hickenbottom, K. L.; Cath, T. Y. Sustainable Operation of Membrane Distillation for Enhancement of Mineral Recovery from Hypersaline Solutions. *J. Membr. Sci.* **2014**, *454*, 426–435.

(23) Duong, H. C.; Gray, S.; Duke, M.; Cath, T. Y.; Nghiem, L. D. Scaling Control during Membrane Distillation of Coal Seam Gas Reverse Osmosis Brine. *J. Membr. Sci.* **2015**, *493*, 673–682.

(24) Gryta, M.; Grzechulska-Damszel, J.; Markowska, A.; Karakulski, K. The Influence of Polypropylene Degradation on the Membrane Wettability during Membrane Distillation. *J. Membr. Sci.* **2009**, *326*, 493–502.

(25) Warsinger, D. M.; Swaminathan, J.; Guillen-Burrieza, E.; Arafat, H. a.; Lienhard V, J. H. Scaling and Fouling in Membrane Distillation for Desalination Applications: A Review. *Desalination* **2015**, *356*, 294–313.

(26) Gryta, M. Long-Term Performance of Membrane Distillation Process. *J. Membr. Sci.* **2005**, *265*, 153–159.

(27) Gryta, M.; Barancewicz, M. Influence of Morphology of PVDF Capillary Membranes on the Performance of Direct Contact Membrane Distillation. *J. Membr. Sci.* **2010**, *358*, 158–167.

(28) Ahmed, F. E.; Lalia, B. S.; Hashaikeh, R. Membrane-Based Detection of Wetting Phenomenon in Direct Contact Membrane Distillation. *J. Membr. Sci.* **2017**, *535*, 89–93.

(29) Kavanagh, J. M.; Hussain, S.; Chilcott, T. C.; Coster, H. G. L. Fouling of Reverse Osmosis Membranes Using Electrical Impedance Spectroscopy: Measurements and Simulations. *Desalination* **2009**, *236*, 187–193.

(30) Barsoukov, E.; Macdonald, J. R. *Impedance Spectroscopy*; John Wiley & Sons, Inc.: Hoboken, NJ, 2005.

(31) Tuberquia, J. C.; Song, W. S.; Jennings, G. K. Investigating the Superhydrophobic Behavior for Underwater Surfaces Using Impedance-Based Methods. *Anal. Chem.* **2011**, *83*, 6184–6190.

(32) Tuberquia, J. C.; Nizamidin, N.; Jennings, G. K. Effect of Superhydrophobicity on the Barrier Properties of Polymethylene Films. *Langmuir* **2010**, *26*, 14039–14046.

(33) Escobar, C. A.; Zulkifli, A. R.; Faulkner, C. J.; Trzeciak, A.; Jennings, G. K. Composite Fluorocarbon Membranes by Surface-Initiated Polymerization from Nanoporous Gold-Coated Alumina. *ACS Appl. Mater. Interfaces* **2012**, *4*, 906–915.

(34) Bannwarth, S.; Breisig, H.; Houben, V.; Oberschelp, C.; Wessling, M. Membrane Impedance Porometry. *J. Membr. Sci.* **2017**, *542*, 352–366.

(35) Gao, Y.; Li, W.; Lay, W. C. L.; Coster, H. G. L.; Fane, A. G.; Tang, C. Y. Characterization of Forward Osmosis Membranes by Electrochemical Impedance Spectroscopy. *Desalination* **2013**, *312*, 45–51.

(36) Ho, J. S.; Low, J. H.; Sim, L. N.; Webster, R. D.; Rice, S. A.; Fane, A. G.; Coster, H. G. L. In-Situ Monitoring of Biofouling on Reverse Osmosis Membranes: Detection and Mechanistic Study Using Electrical Impedance Spectroscopy. *J. Membr. Sci.* **2016**, *518*, 229–242.

(37) Ho, J. S.; Sim, L. N.; Webster, R. D.; Viswanath, B.; Coster, H. G. L.; Fane, A. G. Monitoring Fouling Behavior of Reverse Osmosis Membranes Using Electrical Impedance Spectroscopy: A Field Trial Study. *Desalination* **2017**, *407*, 75–84.

(38) Antony, A.; Chilcott, T.; Coster, H.; Leslie, G. Situ Structural and Functional Characterization of Reverse Osmosis Membranes Using Electrical Impedance Spectroscopy. *J. Membr. Sci.* **2013**, *425–426*, 89–97.

(39) Darestani, M. T.; Chilcott, T. C.; Coster, H. G. L. Electrical Impedance Spectroscopy Study of Piezoelectric PVDF Membranes. *J. Solid State Electrochem.* **2014**, *18*, 595–605.

(40) Coster, H. G. L.; Chilcott, T. C.; Coster, A. C. F. Impedance Spectroscopy of Interfaces, Membranes and Ultrastructures. *Bioelectrochem. Bioenerg.* **1996**, *40*, 79–98.

(41) Coster, H. G. L.; Kim, K. J.; Dahlan, K.; Smith, J. R.; Fell, C. J. D. Characterisation of Ultrafiltration Membranes by Impedance Spectroscopy. I. Determination of the Separate Electrical Parameters and Porosity of the Skin and Sublayers. *J. Membr. Sci.* **1992**, *66*, 19–26.

(42) Sim, V. S. T.; Cen, J.; Chong, T. H.; Yeo, A. P. S.; Krantz, W. B.; Coster, H. G. L.; Fane, A. G. Novel Monitors Enable Early Detection of RO System Fouling. *IDA J. Desalin. Water Reuse* **2012**, *4*, 36–48.

(43) Hoek, E. M. V.; Elimelech, M. Cake-Enhanced Concentration Polarization: A New Fouling Mechanism for Salt-Rejecting Membranes. *Environ. Sci. Technol.* **2003**, *37*, 5581–5588.

(44) Park, J. S.; Chilcott, T. C.; Coster, H. G. L.; Moon, S. H. Characterization of BSA-Fouling of Ion-Exchange Membrane Systems Using a Subtraction Technique for Lumped Data. *J. Membr. Sci.* **2005**, *246*, 137–144.

(45) Tijing, L. D.; Woo, Y. C.; Choi, J. S.; Lee, S.; Kim, S. H.; Shon, H. K. Fouling and Its Control in Membrane Distillation-A Review. *J. Membr. Sci.* **2015**, *475*, 215–244.

(46) Boo, C.; Lee, J.; Elimelech, M. Omniphobic Polyvinylidene Fluoride (PVDF) Membrane for Desalination of Shale Gas Produced Water by Membrane Distillation. *Environ. Sci. Technol.* **2016**, *50*, 12275–12282.

(47) Lee, J.; Boo, C.; Ryu, W. H.; Taylor, A. D.; Elimelech, M. Development of Omniphobic Desalination Membranes Using a Charged Electrospun Nanofiber Scaffold. *ACS Appl. Mater. Interfaces* **2016**, *8*, 11154–11161.

(48) García-Payo, M. C.; Izquierdo-Gil, M. A.; Fernández-Pineda, C. Wetting Study of Hydrophobic Membranes via Liquid Entry Pressure Measurements with Aqueous Alcohol Solutions. *J. Colloid Interface Sci.* **2000**, *230*, 420–431.

(49) Warsinger, D. E. M.; Servi, A.; Connors, G. B.; Mavukkandy, M. O.; Arafat, H. A.; Gleason, K.; Lienhard, J. H., V Reversing Membrane Wetting in Membrane Distillation: Comparing Dryout to Backwashing with Pressurized Air. *Environ. Sci.: Water Res. Technol.* **2017**, *3*, 930–939.

(50) Churaev, N. V.; Martynov, G. A.; Starov, V. M.; Zorin, Z. M. Some Features of Capillary Imbibition of Surfactant Solutions. *Colloid Polym. Sci.* **1981**, *259*, 747–752.

(51) Starov, V. M.; Zhdanov, S. A.; Velarde, M. G. Capillary Imbibition of Surfactant Solutions in Porous Media and Thin Capillaries: Partial Wetting Case. *J. Colloid Interface Sci.* **2004**, *273*, 589–595.

(52) Starov, V. M. Surfactant Solutions and Porous Substrates: Spreading and Imbibition. *Adv. Colloid Interface Sci.* **2004**, *111*, 3–27.

(53) Schick, M. J. Effect of Temperature on the Critical Micelle Concentration of Nonionic Detergents. Thermodynamics of Micelle Formation. *J. Phys. Chem.* **1963**, *67*, 1796–1799.

(54) Schick, M. J. Effect of Electrolyte and Urea on Micelle Formation. *J. Phys. Chem.* **1964**, *68*, 3585–3592.